



*Work is supported by Fermi Research Alliance, LLC, under contract No. DE-AC02-07CH11359 with the U.S. Department of Energy.

Abstract

Nb3Sn magnets with a nominal operation field of 15-16 T are being considered for the LHC energy upgrade (HE-LHC) and a post-LHC Future Circular Collider (FCC). To demonstrate the feasibility of 15 T accelerator quality dipole magnets, the US Magnet Development Program (MDP) is developing a single-aperture 15 T Nb3Sn dipole demonstrator based on a 4-layer graded cos-theta coil with 60 mm aperture and cold iron yoke. The main design challenges for 15 T accelerator magnets include large Lorentz forces at this field level. To counteract them, an innovative mechanical structure based on a vertically split iron yoke, locked by large aluminum IC-clamps and supported by a thick stainless steel skin, has been developed at Fermilab. To study the performance of the structure a parametric multi-physics FEA model has been setup. This paper describes the numerical model as well as the results of a sensitivity analysis of the effect of geometrical tolerances and assembly parameters.

Mechanical Structure

The main features of the 15 T design are illustrated in Figure 1.

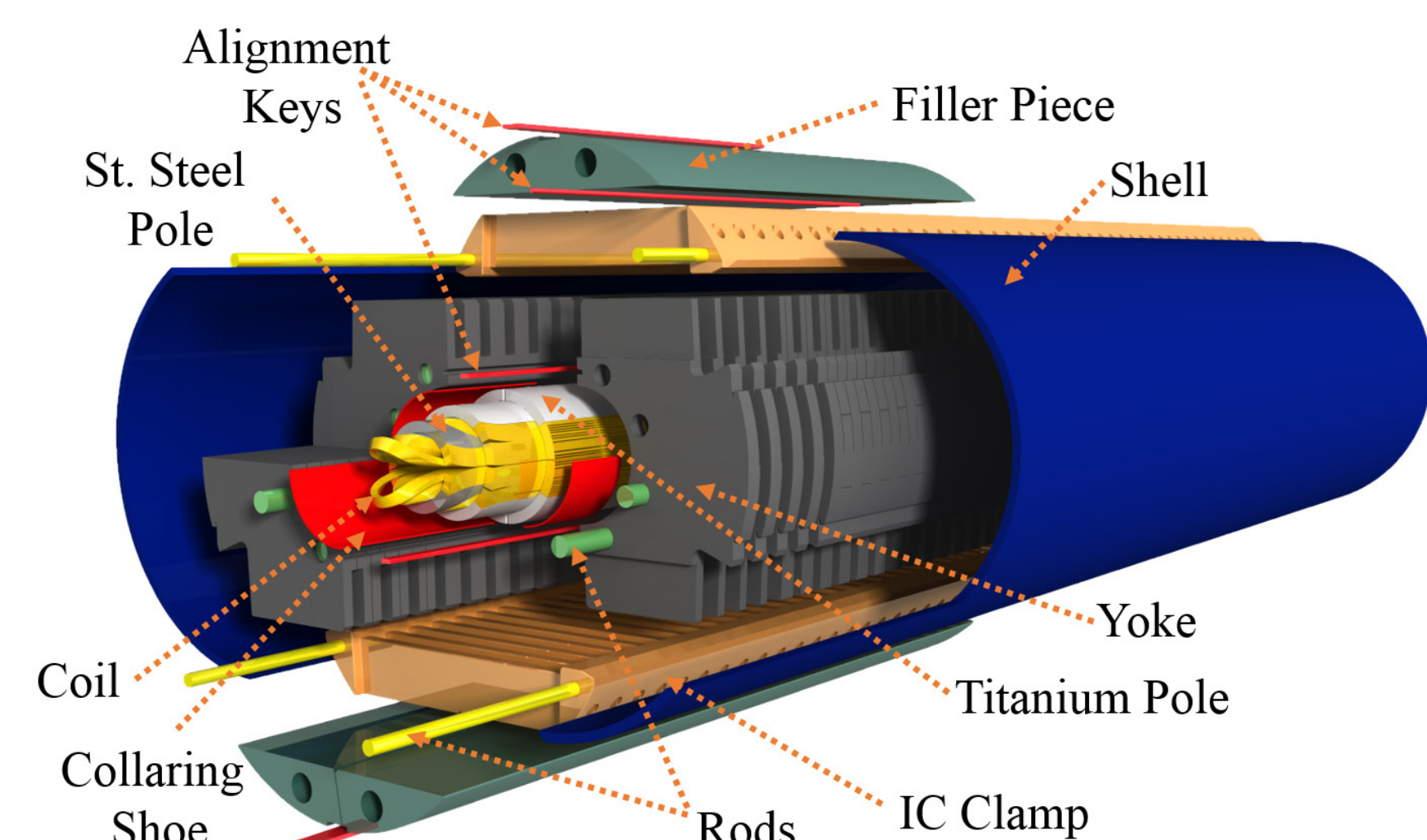


Figure 1. Exploded view of the 15 T Dipole showing the main design features

The coil consists of 4 layers. The two innermost layers (layer 1 & 2) are separated by three wedges, while the two outermost layers (layer 3 & 4) do not use wedges. Titanium poles are impregnated with the layer 1 & 2 of the coil, while layer 3 & 4 is impregnated with St. Steel poles (Figure 2). Aluminum IC-clamps interleave with the iron yoke laminations at their top and bottom sectors, thus reducing the iron filling factor in these areas to ~60% (Figure 2).

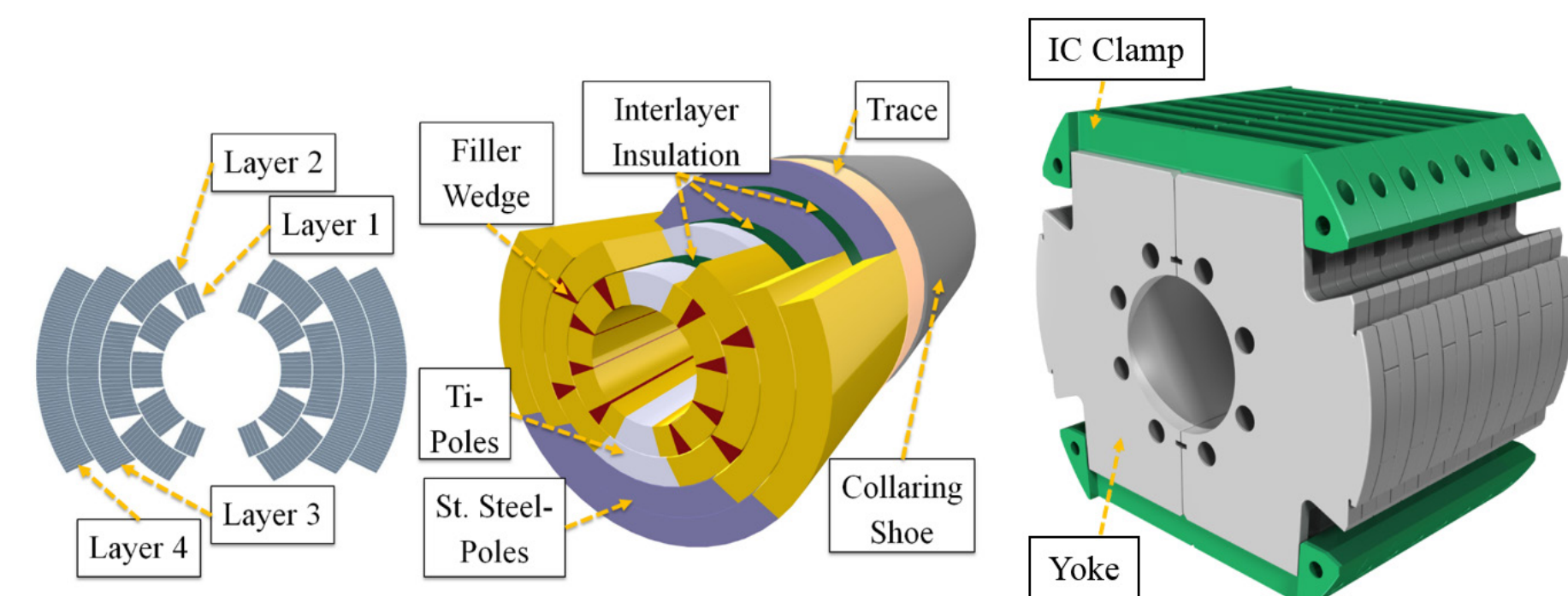


Figure 2. 15T Dipole coil cross section and key features

Design Space & Sensitivity Analysis

The sensitivity analysis is conducted by utilizing the DoE method (Design of Experiments) which determines sampling points used to construct a response surface.

Figure 7 presents the Local Sensitivity Chart regarding Coil Von Mises Stress for the Shimming configuration used to produce the final results. The effect of the variation of shim dimensions was under investigation. Figure 8 presents the effect of the variation of the coil's material properties, namely the Young's Modulus and the Coefficient of Thermal Expansion.

Eleven input parameters (Table 2) were chosen for this study, corresponding to 206 sampling points with the CCD (Central Composite Design) algorithm.

The produced response surface is a full 2nd-order polynomial. The tolerances cover a wide range, leading to a response surface that covers a large design space. Figure 9 presents the response surface of the Coil's max. equivalent stress (MPa) in correlation with the radial coefficient of thermal expansion, α_r (mm/m) and the azimuthal module of Elasticity, E_θ (GPa).

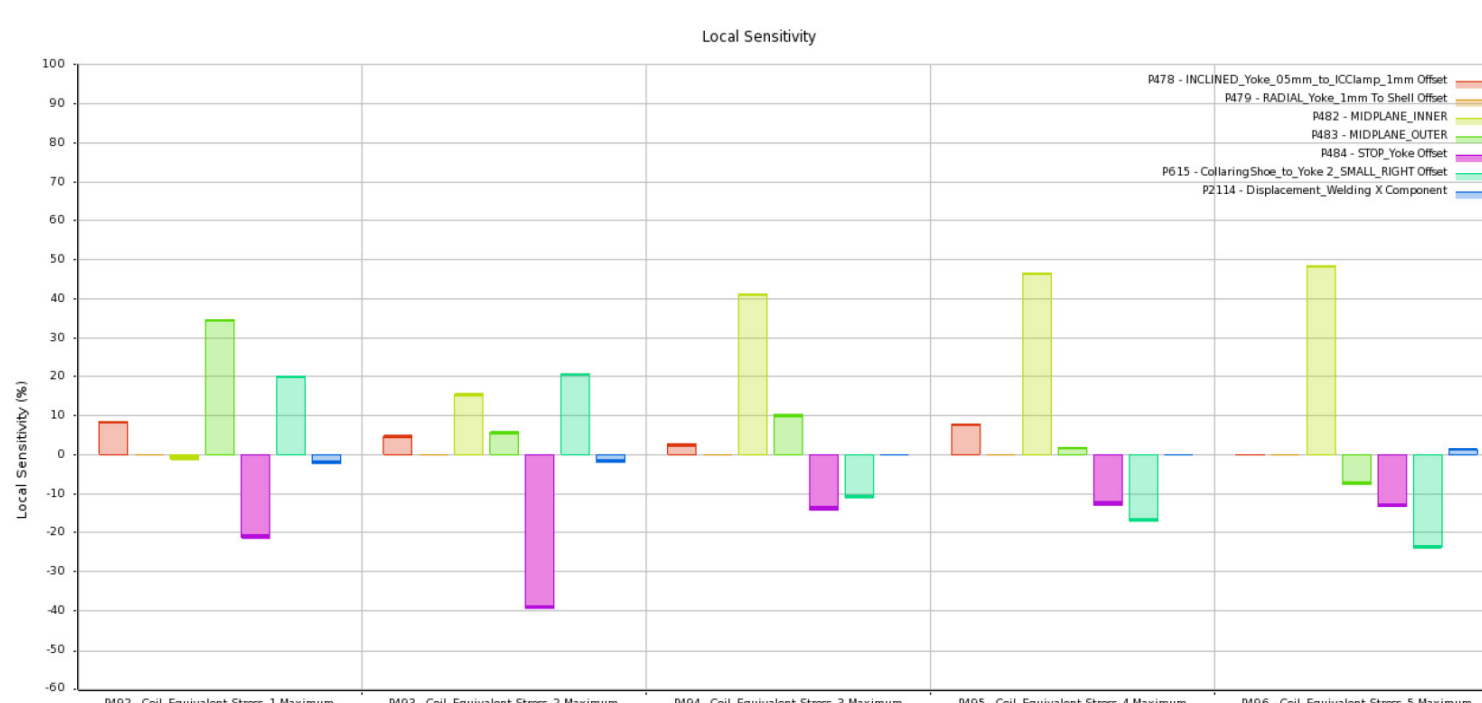


Figure 7. Effect of the variation of shim dimensions on Coil Von Mises Stress

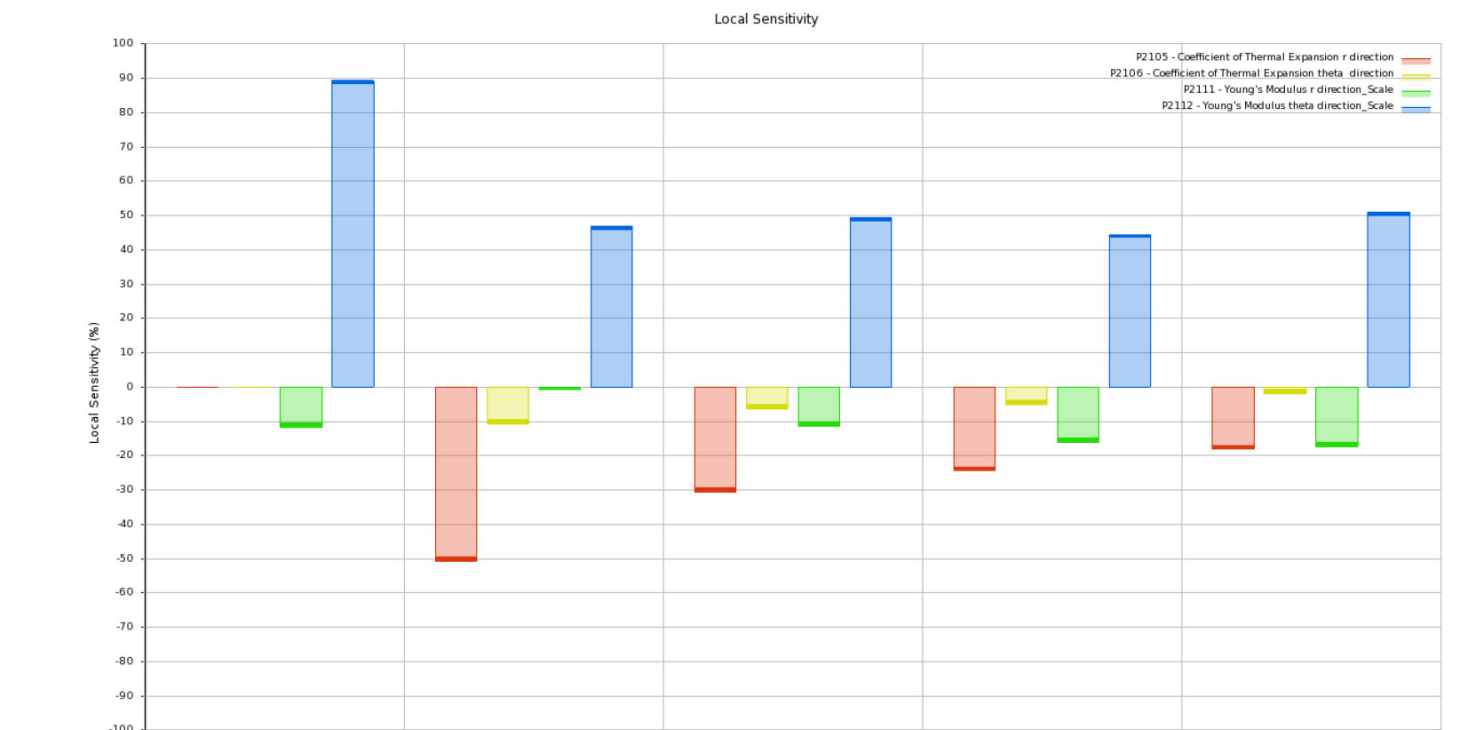


Figure 8. Effect of the variation of the coil's material properties on Coil Von Mises Stress

2D Model

Magnetic Analysis

The electromagnetic model is analyzed in MAXWELL & PITHIA [5] to compare results between the Finite Element (FEM) and the Boundary Element Method (BEM). The magnetic field at 15T is shown in Figure 3 and the Lorentz forces are shown in Table 1.

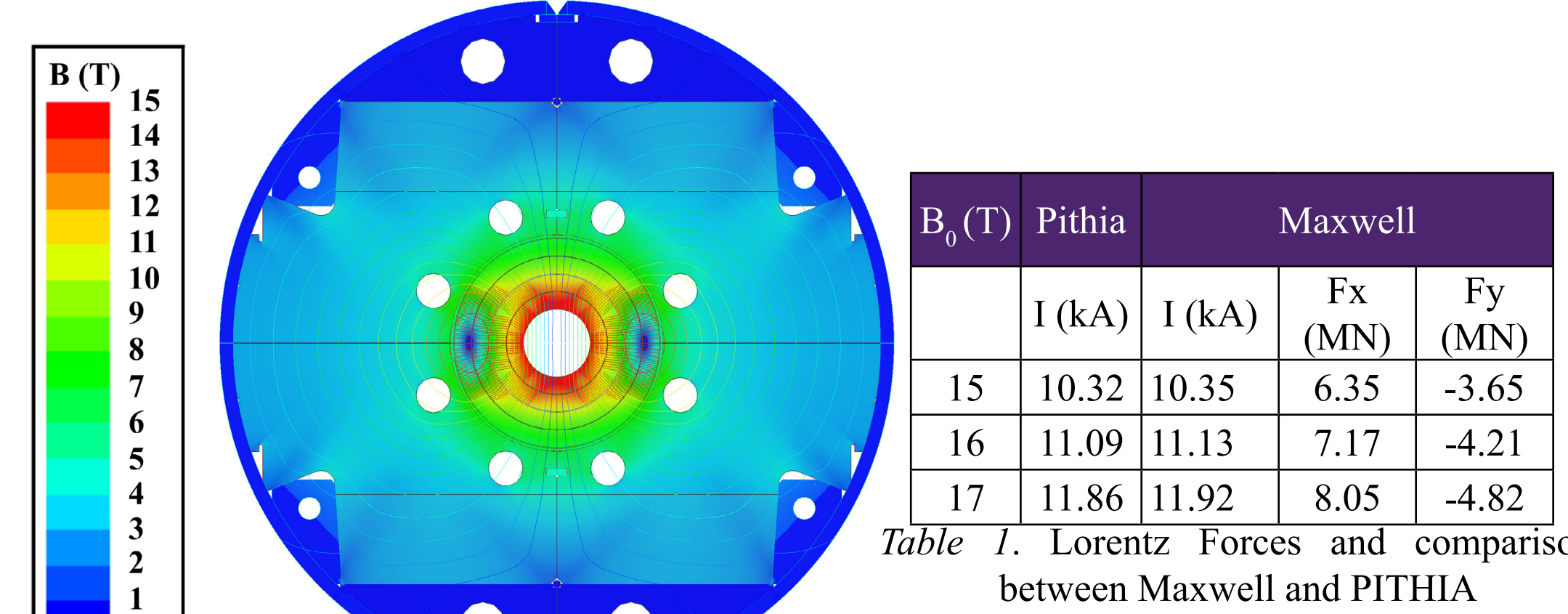


Figure 3. Magnetic field at 15 T

Structural Analysis

A structural analysis was implemented in order to determine the structural integrity of the magnet. Four loadsteps (LS) were considered in the FEM (Figure 4)



Figure 4. Loadsteps

The Von-Mises Coil Stress (MPa) evolution for the four load steps is shown in Figure 5. The stress gradients are smooth and very symmetric and the peak stress remains below 200 MPa up to 16 T. The difference in radial deformation of the midplane between two sequential load-steps of layer 1, 2, 3 and 4 is presented in Figure 6.

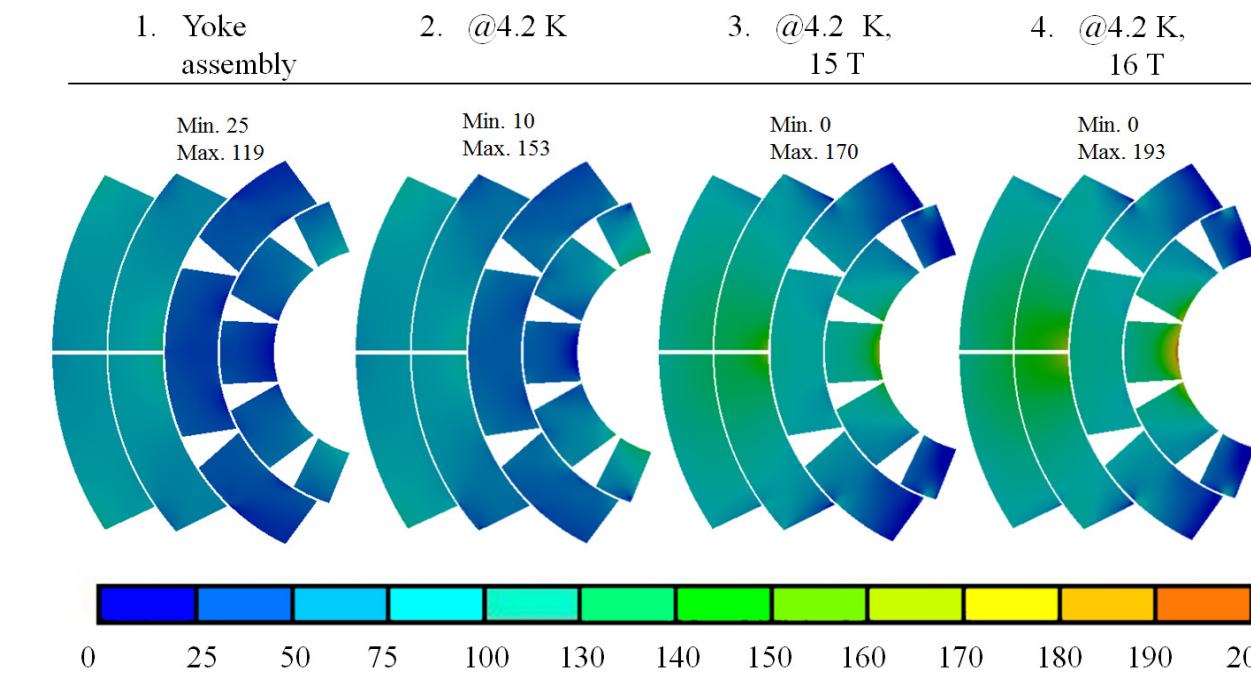


Figure 5. Von-Mises Coil Stress (MPa) evolution

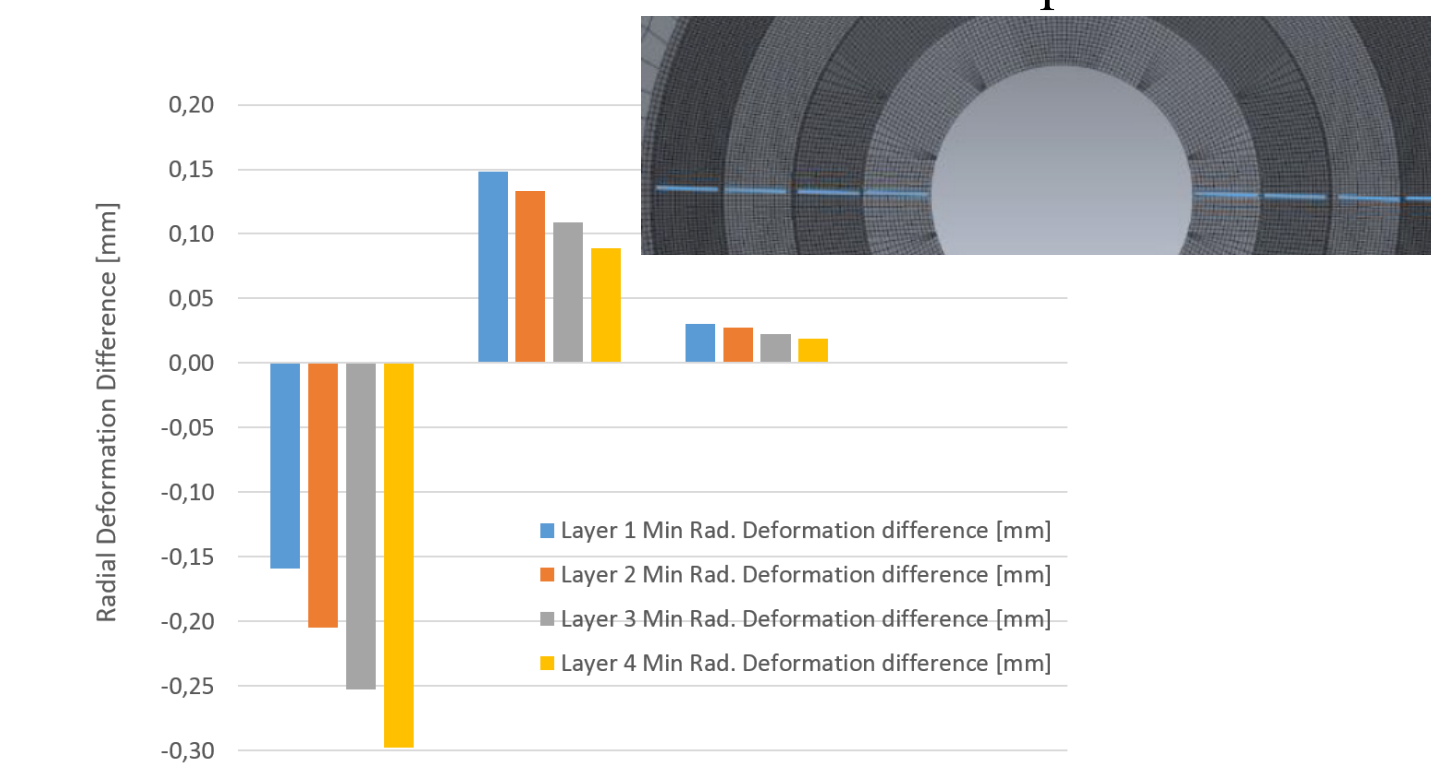
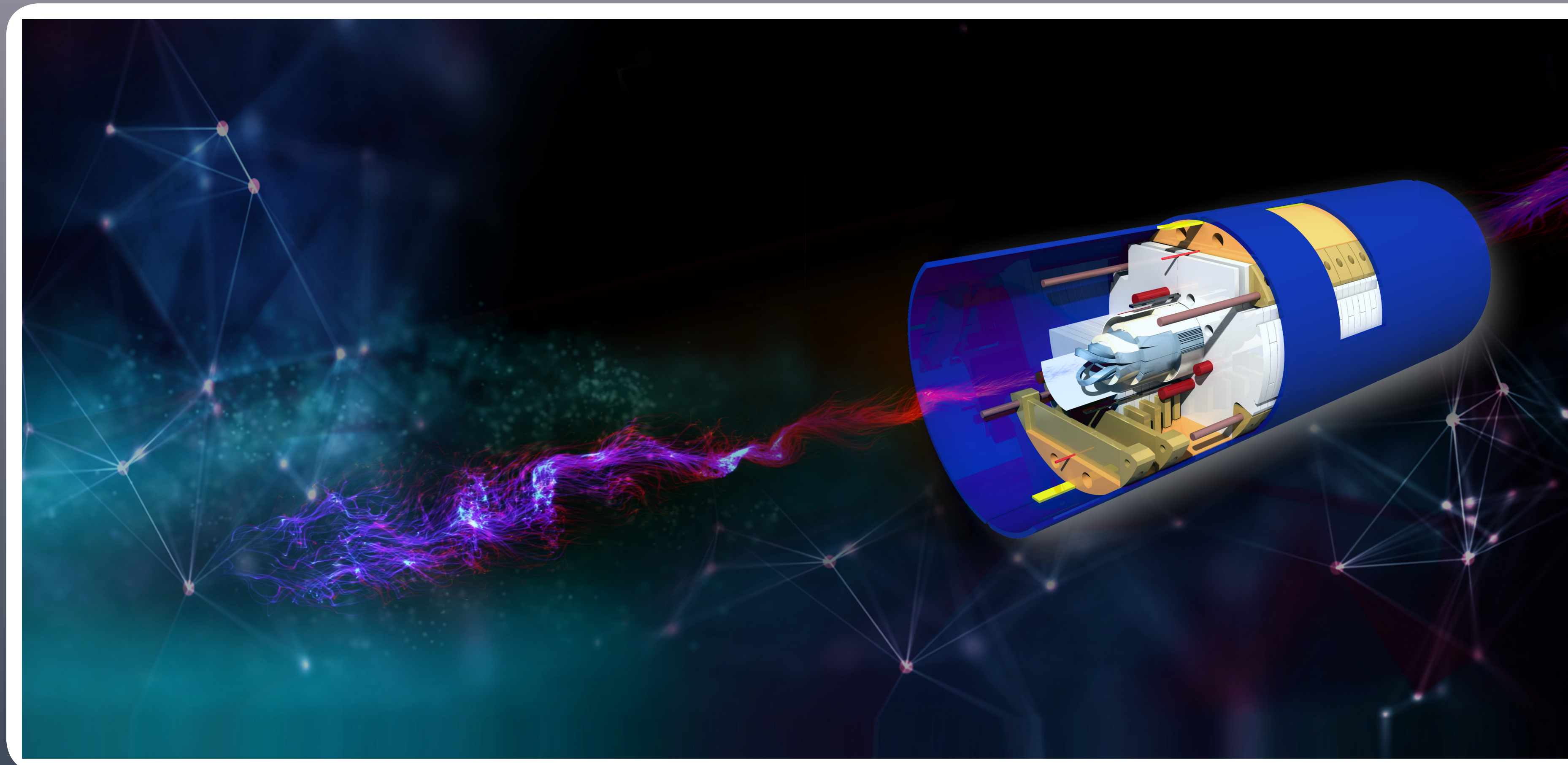


Figure 6. Difference in radial deformation of the midplane between two sequential load-steps



Conclusions

The sensitivity analysis regarding the impact of the variation of shim dimensions on Coil Von Mises Stress showed that:

- During LS1 (assembly) the outer midplane shim and the Coil-Yoke shim have the largest impact on the coil stress. The mid-plane shim exerts pressure on the coil in the azimuthal direction and the coil-yoke one in the radial direction. The thicker the shims are, the more pressure is exerted on the coil, hence the positive correlation. The coil is deformed elliptically along the vertical axis as a result of this shimming. For the tapered shim at the yoke-yoke interface there is a limit imposed on the thickness due to the specification that the Yoke gap shall remain open at room temperature. A thick shim reduces the coil stress but will close the gap.
- During LS2 (cooldown) the yoke-yoke shim and the Coil-Yoke shim have the largest impact on the coil stress. The location of maximum equivalent stress changes from the third layer to the first. The impact of the outer mid-plane shim is diminished and the inner mid-plane shim is more impactful on the coil stress, again with a positive correlation. The coil-yoke shim continues to be important. The shim with the highest impact on coil stress is the tapered Yoke shim. At cold, the yoke gap closes and the yoke becomes a rigid envelop for the coil.
- During LS3 & LS4 (powering) the inner midplane shim becomes the more impactful one, as max stress continues to appear on the first layer of the coil. The coil-yoke shim now has a negative impact on coil stress. As the coil is deformed by the Lorentz forces, being ovalized along the horizontal axis, the coil-yoke shim counteracts this, pushing the coil towards the vertical axis, limiting the deformation and stress. The outer mid-plane shim's impact is positive at 15T, as an area of high stresses appears in the third layer. At 16 T the high stresses are removed from that area and the outer mid-plane shim's impact is decreased. The tapered Yoke shim still has a negative correlation with Coil stress, although it is reduced. This is explained because the gap is closed and the yoke's rigidity remains stable.
- The Yoke-Clamp and Yoke-Shell shims, as well as the displacement simulating the welding have much lower sensitivities than the rest of the shims in the range of variation that was imposed on them.
- During LS3 & LS4 (powering) the coil's Coil Von Mises Stress remains below 200 MPa.
- During LS1 (assembly) the yoke gap remains open while in LS2, LS3 and LS4 it is closed.

The sensitivity analysis regarding the impact of the variation of the coil's material properties on Coil Von Mises Stress showed that:

- During LS1 (assembly) E_θ has the largest impact on coil stress, as thermal expansion is not taking place yet. As the structure is shimmed, the coil is ovalized along the vertical axis. Because of this ovalization and the pressure exerted by the outer mid-plane shim on the coil in the azimuthal direction, variations of E_θ are much more important than those of E_r .
- During LS2 (cooldown) the effect of the coefficients of thermal expansion becomes apparent. The coil shrinks, mainly along the radial direction. This can be observed by the high impact of α_r , which has the largest sensitivity in this load step. As α_r increases the coil contracts more and the pressure exerted upon it from the rest of the structure lessens. This causes a decrease in coil stress. At the same time, E_θ maintains a decreased but still high impact on coil stress as the ovalization of the coil lessens and it becomes more circular.
- During LS3 & LS4 (powering) the sensitivity of α_r remains relevant since the structure remains at a cryogenic temperature but decreases as the Lorentz forces increase. The main input remains E_θ as the magnetic forces change the ovalization of the coil, deforming it along the horizontal axis. This deformation is connected with the steady increase of the sensitivity of E_r throughout powering. The majority of the magnetic forces act along the horizontal axis. The radial orientation of the coil is more along the X axis, less along the vertical plane. So as the magnetic forces become stronger, the radial value of E becomes more relevant.

References

- [1] A.V. Zlobin et al., "Design concept and parameters of a 15 T Nb3Sn dipole demonstrator for a 100 TEV Hadron Collider", IPAC, Richmond, May 2015
- [2] V. V. Kashikhin et al., "Magnetic and structural design of a 15 T Nb3Sn accelerator dipole model", CERN, Tucson, July 2015
- [3] I. Novitski et al., "Development of a 15 T Nb3Sn accelerator dipole demonstrator at Fermilab", MT 24, Seoul, October 2015
- [4] I. Novitski et al., "Development and comparison of mechanical structures for FNAL 15 T Nb3Sn accelerator dipole demonstrator", NAPA, November 2016
- [5] PITHIA BEM software package, www.feacomp.com/pithia
- [6] T. Gortsas, et al., "An advanced ACA/BEM for solving 2D large-scale problems with multi-connected domains", CMES: Computer Modeling in Engineering & Sciences, 107(4), pp. 321-343, 2015
- [7] C. Kokkinos et al., "The Short Model Coil (SMC) Nb3Sn Program: FE Analysis with 3D Modeling", IEEE Trans. Appl. Supercond., Vol. 22, No. 3, June 2012.
- [8] M. Karpinen et al., "Design of 11 T Twin-Aperture Nb3Sn Dipole Demonstrator Magnet for LHC Upgrades", MT 22 Marseille, September 2011

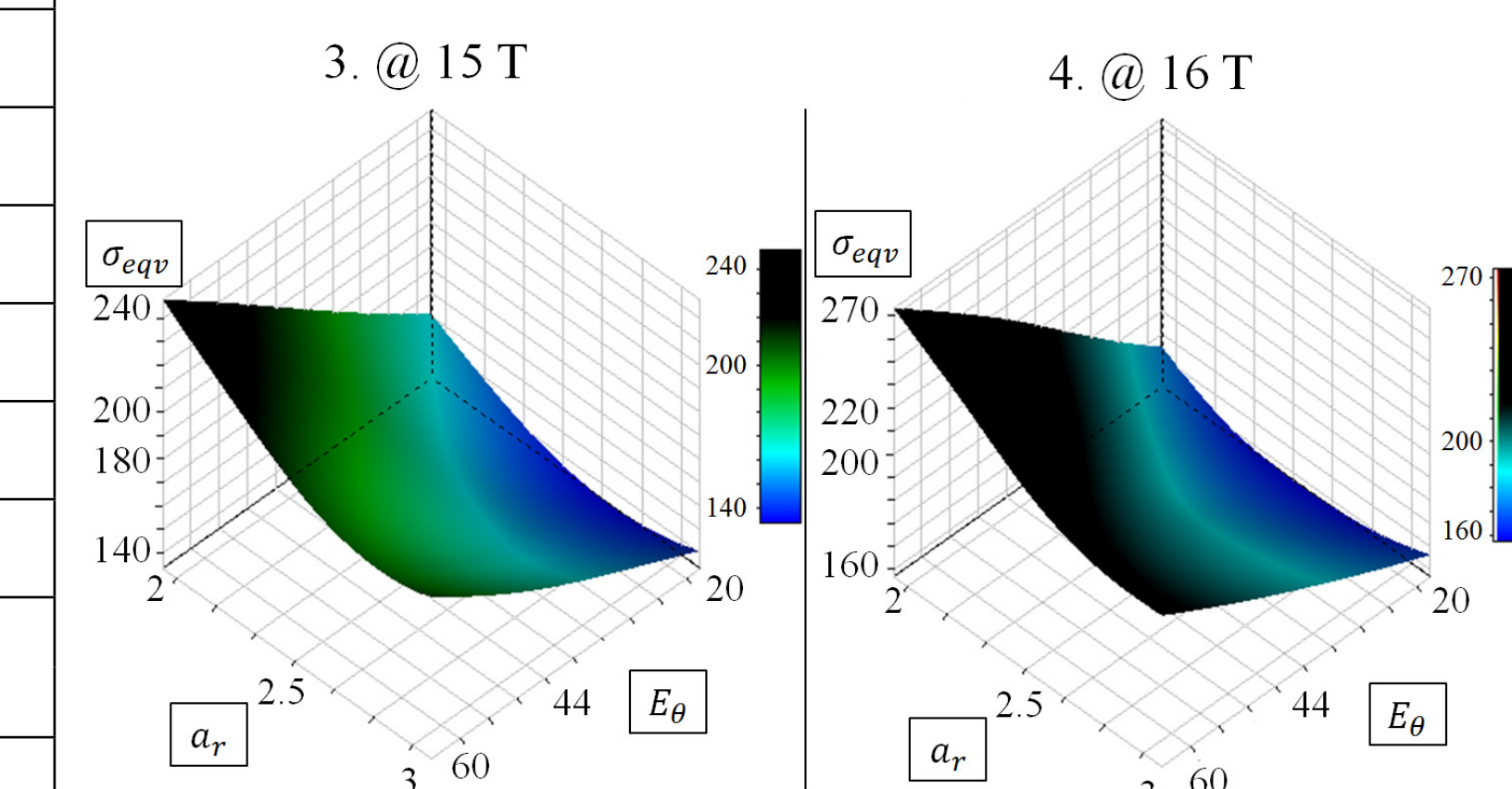


Figure 7. Response surface of the Coil's max. equivalent stress in correlation with α_r and E_θ

Parameter	Nominal Value	Range	Coil-Von Mises	Coil-Von Mises	Coil-Von Mises	Coil-Von Mises				
			@ 293K (119 MPa)	@ 4.2K (153 MPa)	@ 15T (170 MPa)	@ 16T (193 MPa)				
			Range $\Delta \sigma_{max}$ [MPa]							
Weld shrinkage	0.4 mm	0-0.06	117-120	3	152-154	2	170-171	1	192-194	2
MP Inner (1)	0	0-0.09	109-119	17	153-179	26	170-218	48	193-241	48
MP Outer (2)	0.06 mm	0-0.06	102-145	43	151-162	11	170-196	26	192-205	13
Yoke - Yoke (3)	0.36 mm	0.5-0.65	103-120	17	128-178	50	167-177	10	189-199	10
Yoke - Shell (4)	0.6 mm	0.35-0.45	118-120	2	152-154	2	170-171	1	192-194	2
Yoke - IC Clamp (5)	0.4 mm	0.31-0.41	113-123	10	152-155	3	170-171	1	191-195	4
Collaring Shoe - Yoke (6)	0.025 mm	0.35-0.45	119-138	19	143-178	35	170-180	10	183-205	22
E_r	44GPa @ RT	20-60 GPa	118-124	6	153-154	1	170-187	17	188-214	26
E_θ	55GPa @ 4.2K	25-77 GPa	100-141	41	17-177	80	136-199	63	157-226	69
α_r	44GPa @ RT	20-60 GPa	119-119	0	126-126	90	168-213	45	193-234	41
α_θ	2.6 mm/m	2-3 mm/m	119-119	0	143-163	20	164-177	13	190-198	8

Table 2